

Ion Bernstein Wave Heating: a Tool to Modify the Plasma Profile

Benoit P. LeBlanc

Princeton Plasma Physics Laboratory

41st Meeting of the American Physical Society -
Division of Plasma Physics

November 15-19, 1999

Seattle, WA

Motivation

- Active control of pressure profile needed for bootstrap current alignment in advanced tokamak and reactor.
 - Workshop on the Physics for AT's, (San Diego, 1999)
 - Snowmass, July 1999
- Suppress turbulent transport locally, by creating a *sheared* poloidal motion driven by IBW's $\langle \tilde{\mathbf{E}} \times \mathbf{B} \rangle$.
 - Biglari, *et al.*, RF Power in Plasmas, 9th Topical Conf., AIP Conf. Proc. 244, p.376 (1991)
 - C.G. Craddock and P.H. Diamond, Phys. Rev. Lett. **67**, 1536 (1991)

Outline

- PBX-M results
 - internal transport barrier observed (1992-1993)
- Physical picture
 - poloidal drive
 - multi-species effects
- TFTR results
 - poloidal velocity shearing observed during IBW (1997)
- FTU results
 - Internal barrier and heating/ITB observed
- Conclusion

Notation time average $\langle A \rangle \rightarrow A$

IBW on PBX-M: Internal Transport Barrier Observed on **all** kinetic profiles

- $5\Omega_D$, 55 MHz, 300 kW, 1.5 T
- When applied to an H-mode plasma, obtained an internal transport barrier,
- observable on profiles T_e , n_e , T_i , and v_ϕ

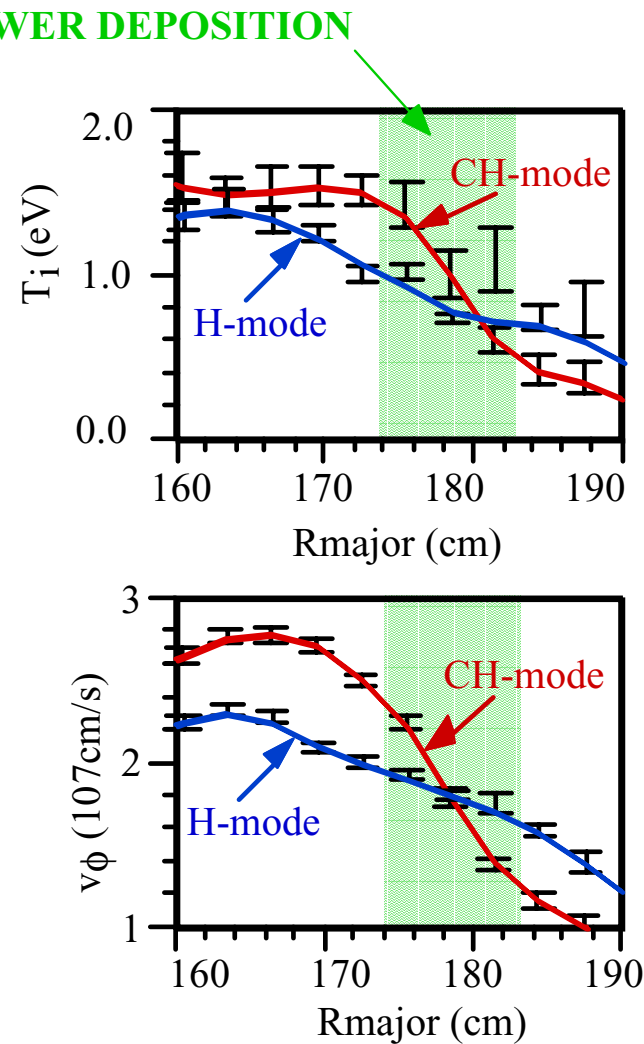
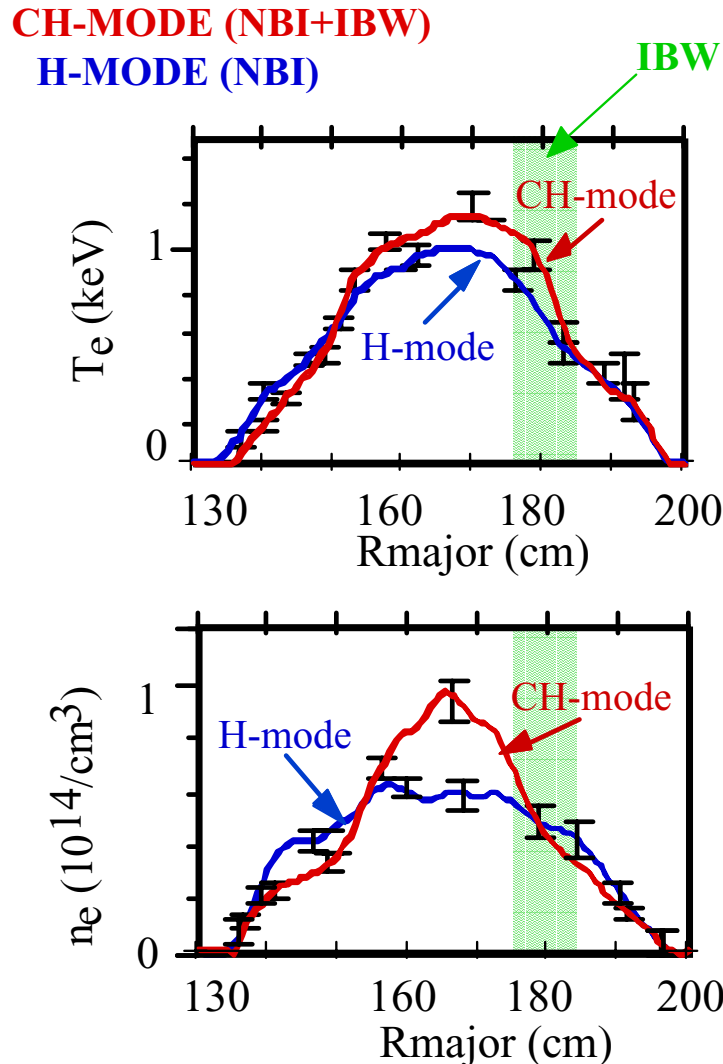
R. Kaita IAEA 1992

B. LeBlanc APS 1993

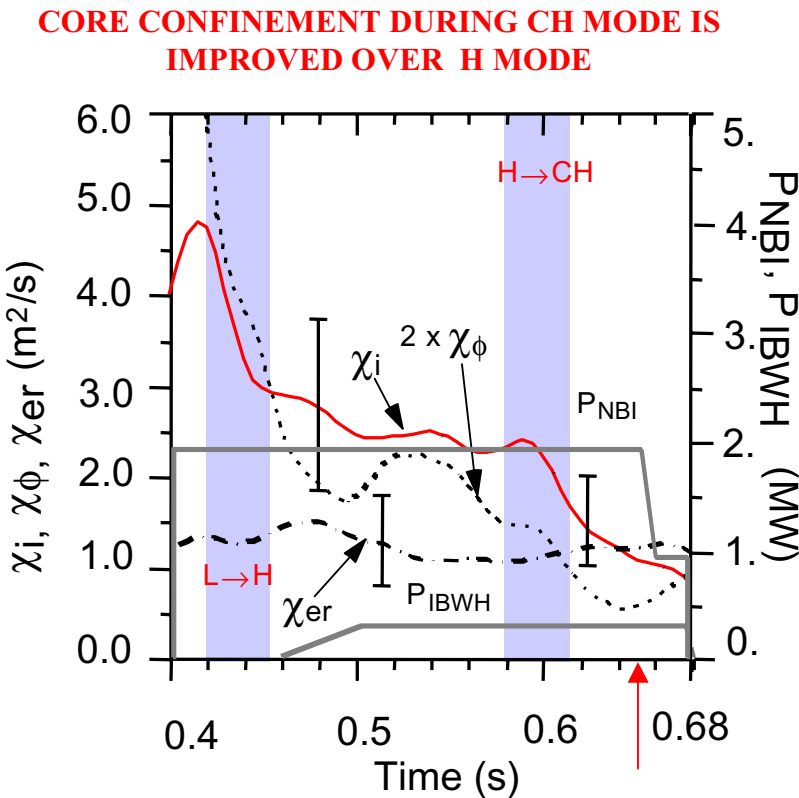
M. Ono, IAEA 1994,

B. LeBlanc, PoP 1995

Barrier Coincides with IBW Power Deposition

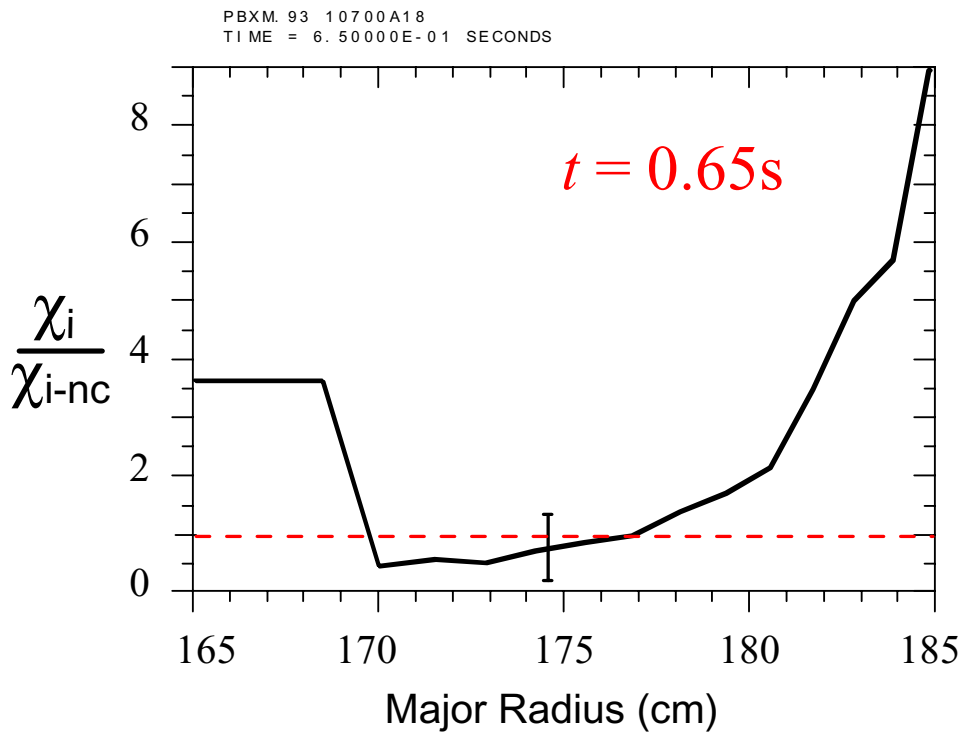


Neoclassical Confinement Obtained at Barrier Location during CH Mode



Volume average over $0.3 < r/a < 0.45$.

TRANSPORT FALLS TO NEOCLASSICAL LEVEL DURING CH MODE



B. LeBlanc, PoP ,2, 741 (1995)

CH Mode Reminiscent of Other Internal Barrier Modes

- Sharp gradients within the plasma column
- Neoclassical confinement at the internal barrier location
- Flat temperature profile inside internal transport barrier

IBW-Induced Reynolds Stress Generates Poloidal Flow

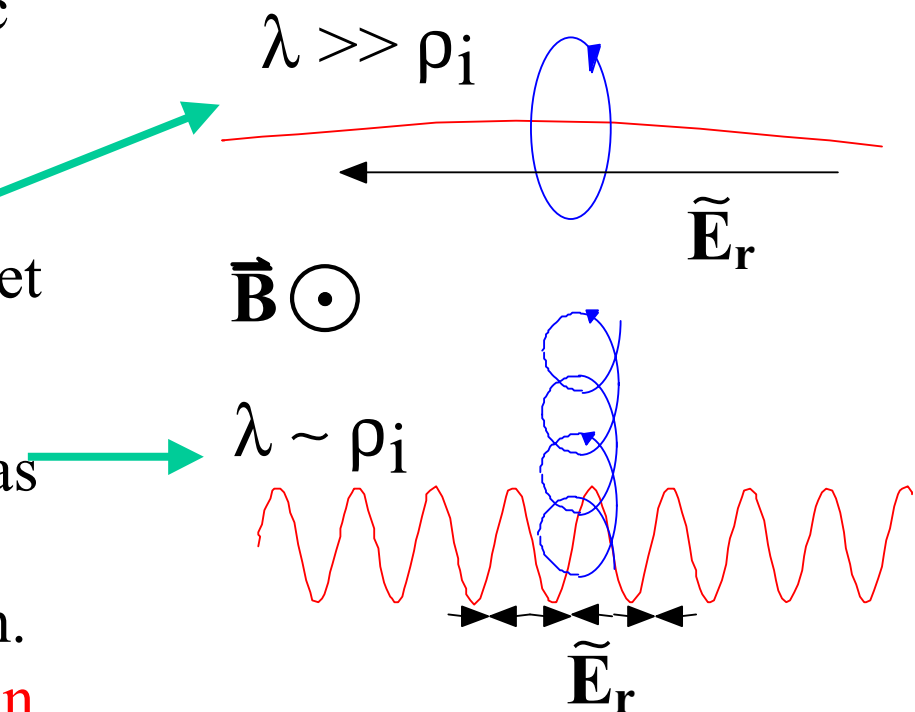
$$\rho_m \left[\tilde{V} \cdot \nabla \tilde{V}_\theta + \mu_{neo} V_\theta \right] = \tilde{\rho}_q \tilde{E}_\theta + \frac{1}{c} (\tilde{J}_x \tilde{B})_\theta$$

Reynolds Stress neoclassical damping Charge-separation induced flow Electromagnetic correction
IBW Dominant for IBW Normally ignored (small)

$$\frac{dV_\theta}{dr} = -\frac{d}{dr} \left[\frac{\tilde{V} \cdot \nabla \tilde{V}_\theta}{\mu_{neo}} \right] > C_s/R \text{ for turbulence suppression}$$

Short Wavelength and E_r Lead to Poloidal Flow

- Consider wave with ω near resonance and radial electric field E_r .
- Long wavelength ($\lambda \gg \rho_i$) elongates gyro motion, no net drift.
- Short wavelength ($\lambda \sim \rho_i$) has ratcheting effect on ion motion, in poloidal direction.
Proper phasing in time and in space insures motion.
- Single pass absorption



IBW's Unique Combination of High E_{\perp} and k_r Induces Strong Poloidal Flow

$$V_{\theta\sigma} = \frac{1}{\mu_{neo}} (\tilde{V} \cdot \nabla \tilde{V}_{\theta})_{\sigma} \cong \frac{1}{\mu_{neo}} \sum_{rays-j} a_{\sigma} b_{\sigma} \tilde{E}_{\perp j}^2 k_{r,j} \operatorname{sgn}(k_r)$$

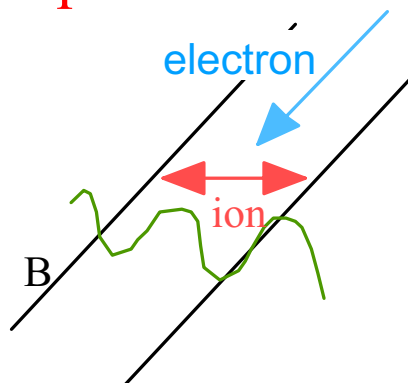
→ $a_{\sigma} = (c\Omega_{\sigma} / B_o k_{\parallel} V_{T\sigma}) \sum_{n=1}^{\infty} (n^2 e^{-\lambda} I_n) [Z_0(y_n) + Z_0(y_{-n})]$

$$b_{\sigma} = (c\Omega_{\sigma} / B_0 k_{\parallel} V_{T\sigma}) \sum_{n=1}^{\infty} [ne^{-\lambda} (I_n - I_{-n})] [Z_0(y_n) - Z_0(y_{-n})]$$

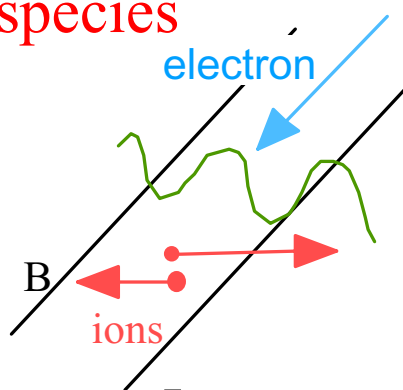
Where $V_{\theta\sigma}$ the poloidal velocity for species “ σ ” and a_{σ} and b_{σ} are the polarization and ExB response functions.

Multi-species Effects Can Lead to Increased Susceptibility

One species



Two species



*Larger motions
Opposite directions*

Response function

$$a_i \propto \chi_i \cong K_{xx} \cong n_{\parallel\parallel}^2 \text{ (small)}$$

Susceptibility

$$\chi_1 + \chi_2 \cong K_{xx} \cong n_{\parallel\parallel}^2$$

$$|\chi_1| \text{ and } |\chi_2| \gg n_{\parallel\parallel}^2$$

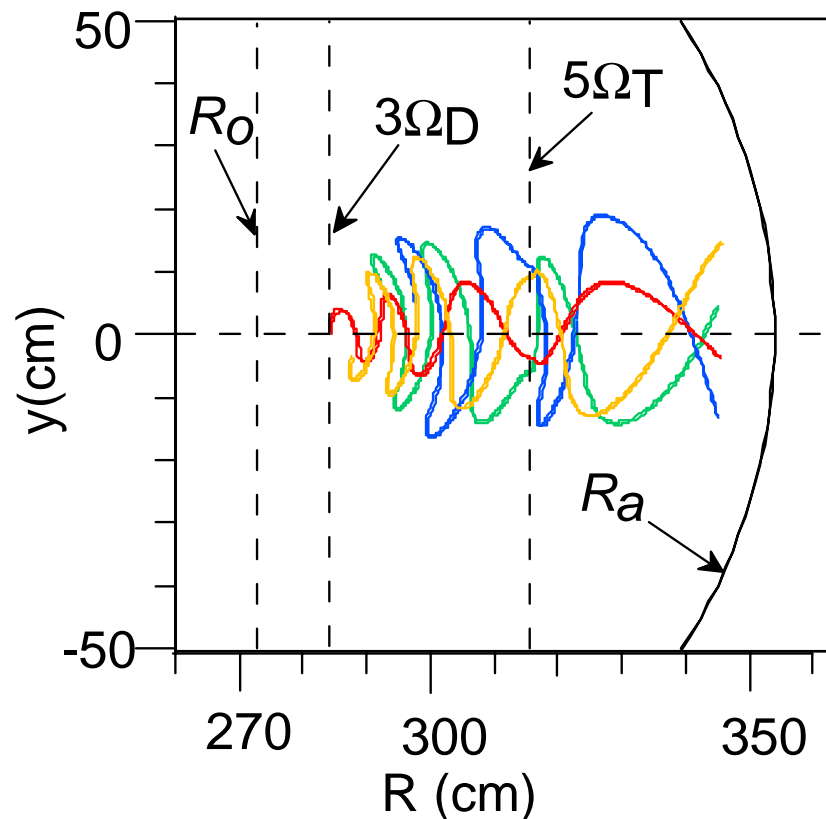
Dielectric tensor

Antenna

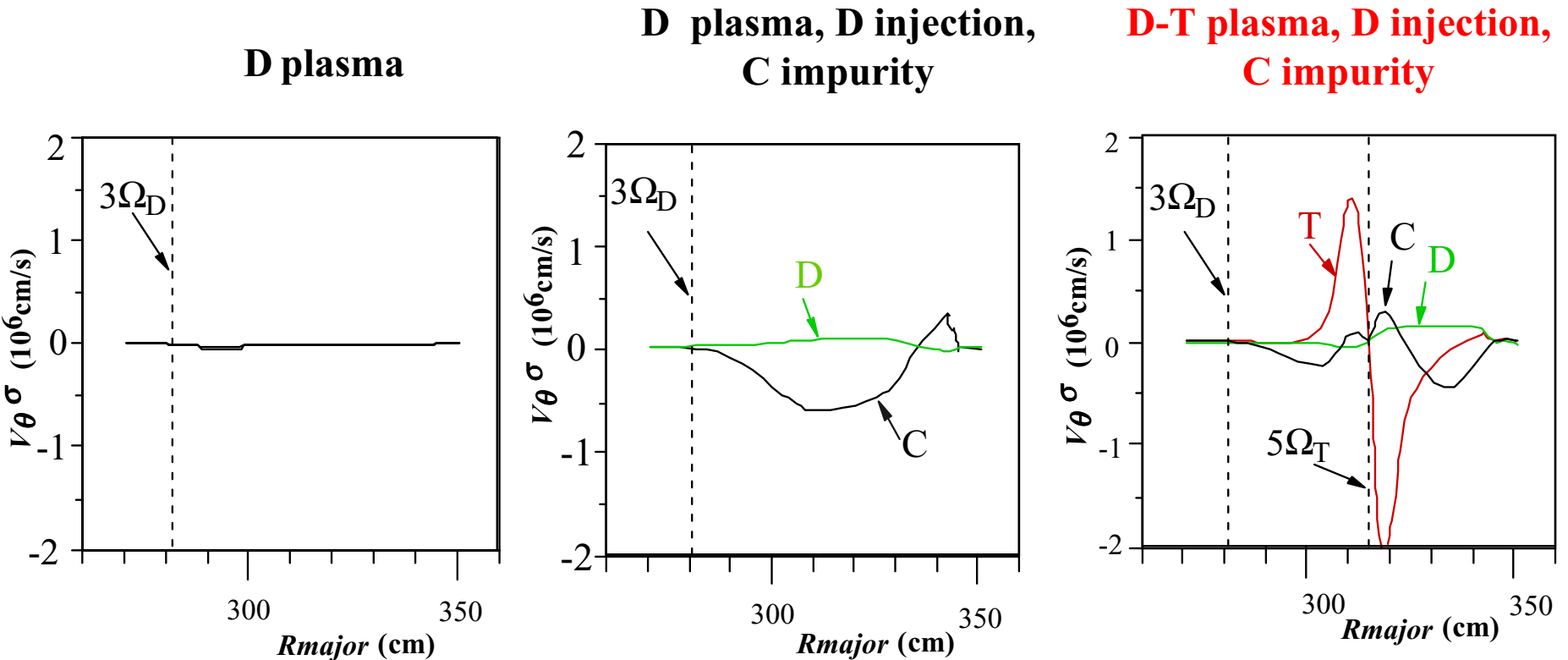
M. Ono, RF Conf, Palm Spring, 1995

IBW Power Deposition and V_θ Computed by Ray Tracing

- Four out of 40 rays typically used for computation are seen.
- Reads in TRANSP species profiles.
- Compute a_σ and b_σ response functions and solve for V_θ .



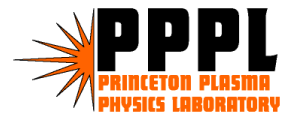
Drive Depends on Plasma Composition



- Higher shear with D-T plasma
- Measure V_θ^c

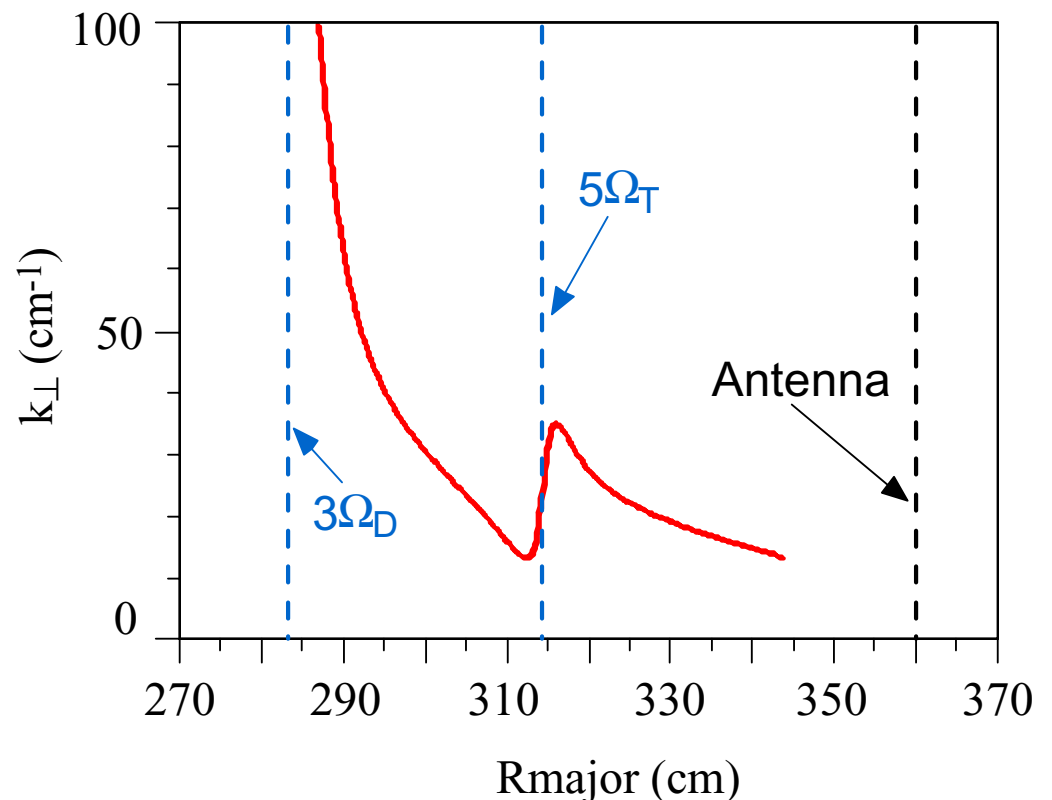


LeBlanc/APS99/ 13

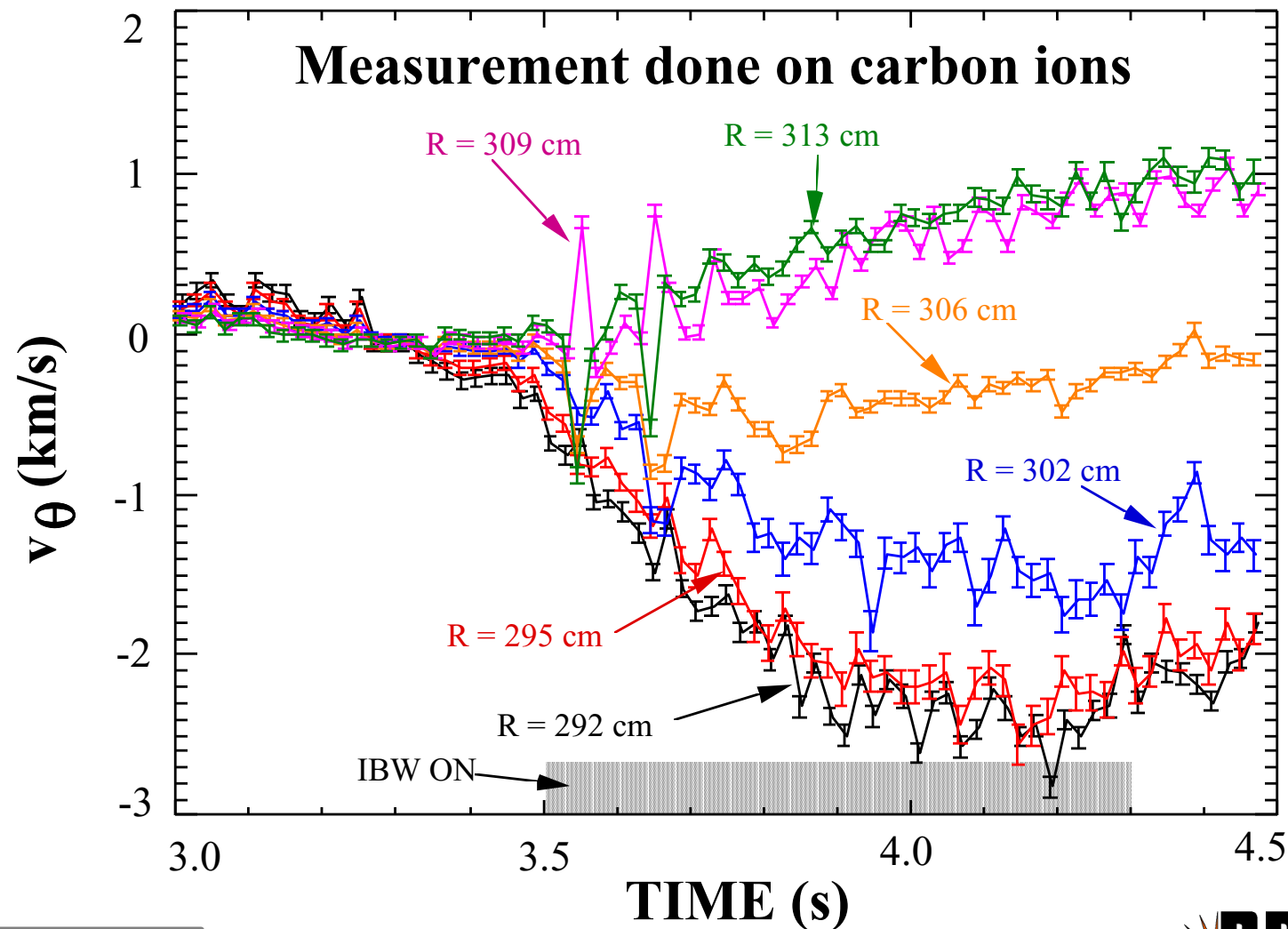


Direct-Launch IBW Experiment In TFTR

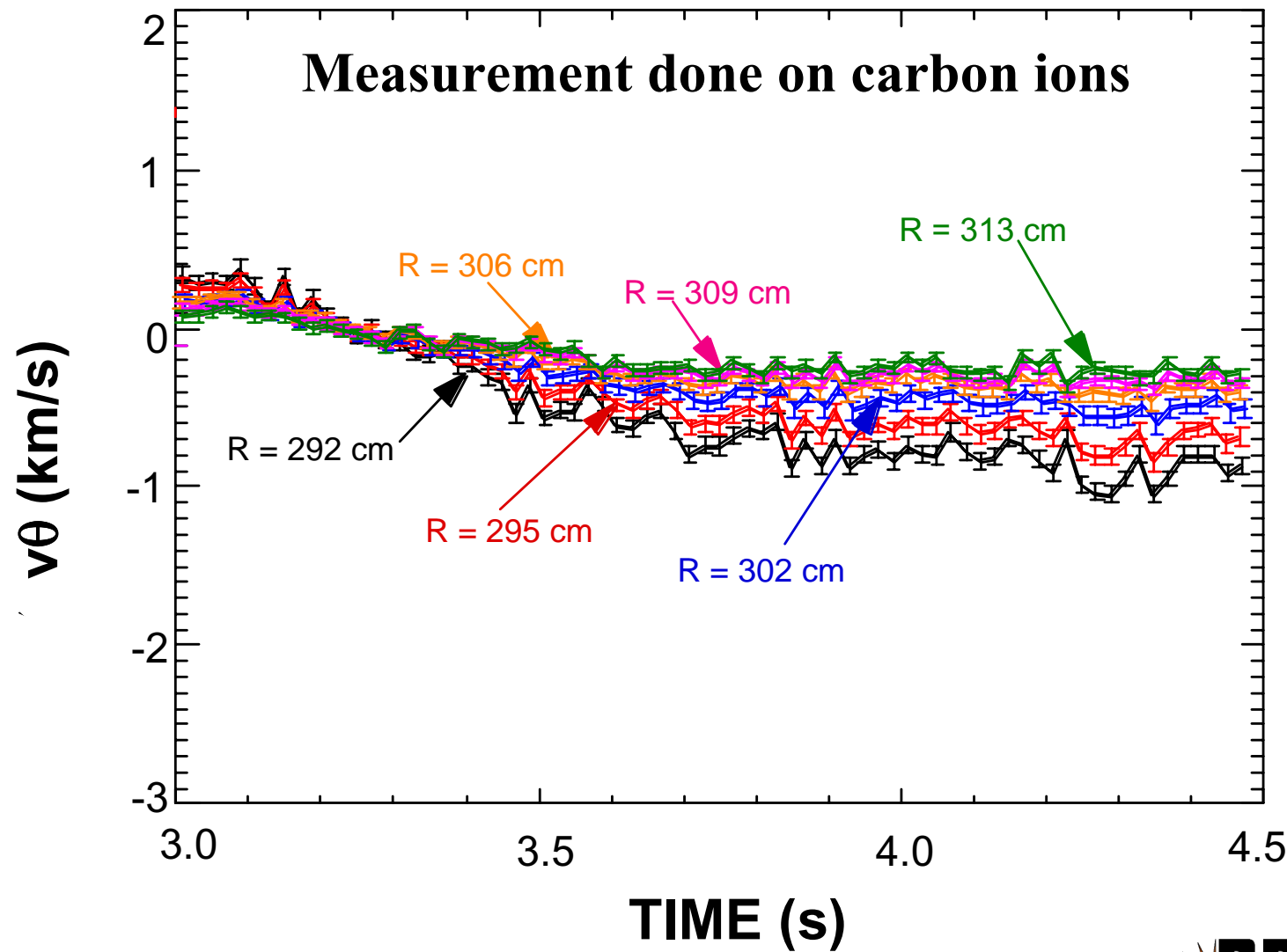
- 76 MHz, 3.45 T, \approx 400 kW
- $5\Omega_T$ and $3\Omega_D$ layers inside plasma
- Tritium Wall Fueling
- Carbon-impurity poloidal velocity measurement



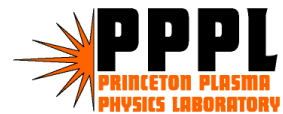
Sheared Poloidal Flow Develops during IBW Heating



Small Residual Sheared Flow without IBW

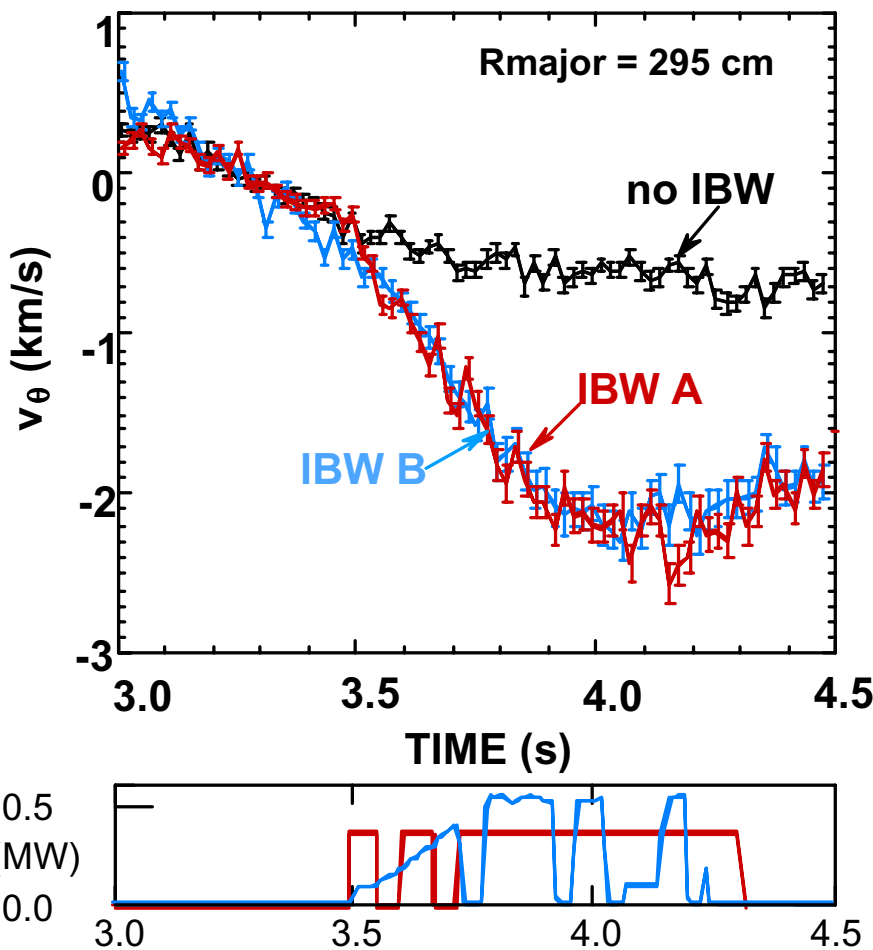


LeBlanc/APS99/ 16

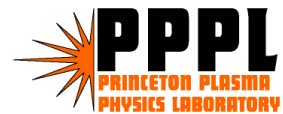
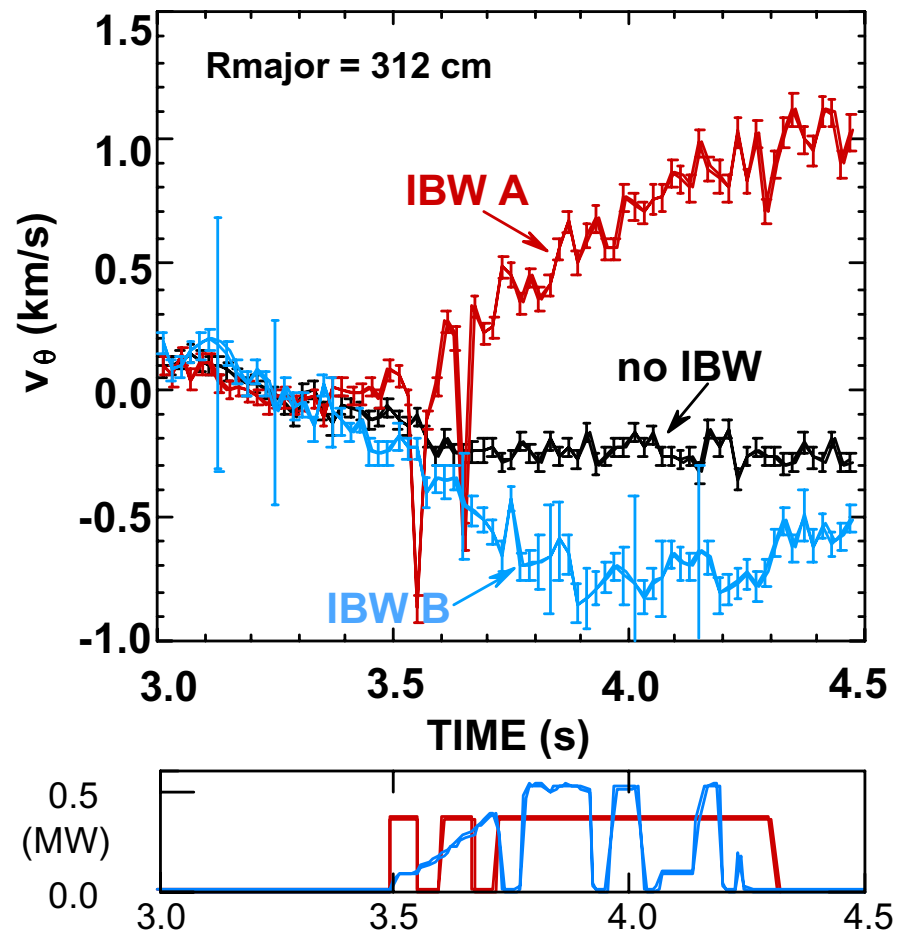


Tritium Density Determines V_θ

Negative Δv_θ observed between $3\Omega_D$ and $5\Omega_T$ layers, for IBW A and IBW B.

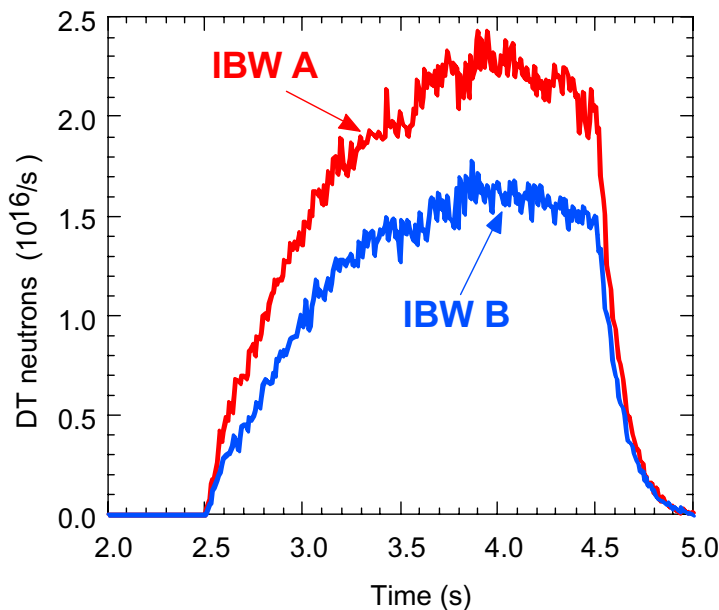


Positive Δv_θ observed near $5\Omega_T$ for case IBW A, while Δv_θ is negative for IBW B.

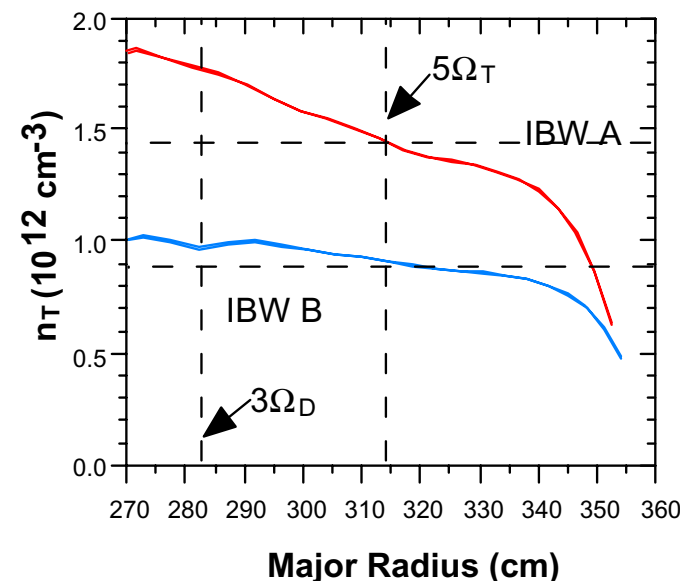


Different Species Mix

More Tritium in A than B



Experimental DT neutrons showed that plasma IBW A had higher tritium content.

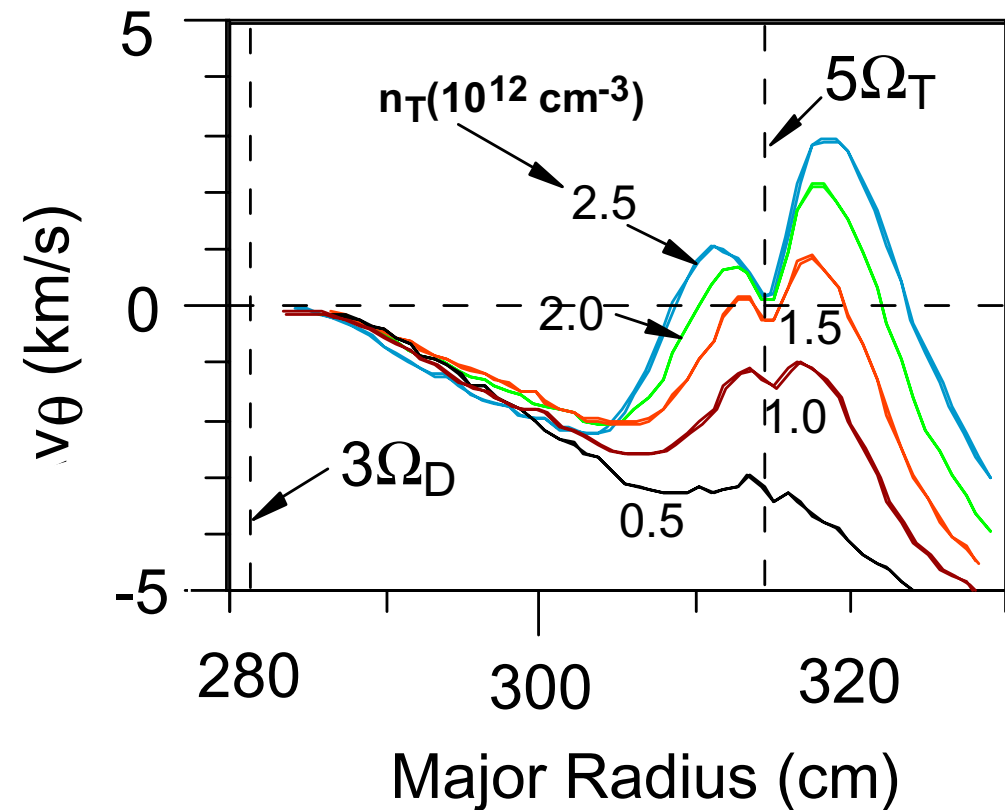


TRANSP analyses indicate that IBW A had 50% more tritium density at the $5\Omega_T$ resonance location.



IBW Ray Tracing Reproduces Experiment

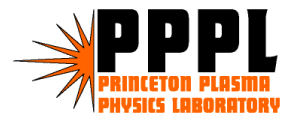
- The Δv_θ drive in the vicinity of the $5\Omega_T$ layer is strong function of n_T .
- Negative drive on the high-field side of $5\Omega_T$ is insensitive to n_T .



B. LeBlanc, Phys. Rev. Lett. 82, 331 (1999)



LeBlanc/APS99/ 19

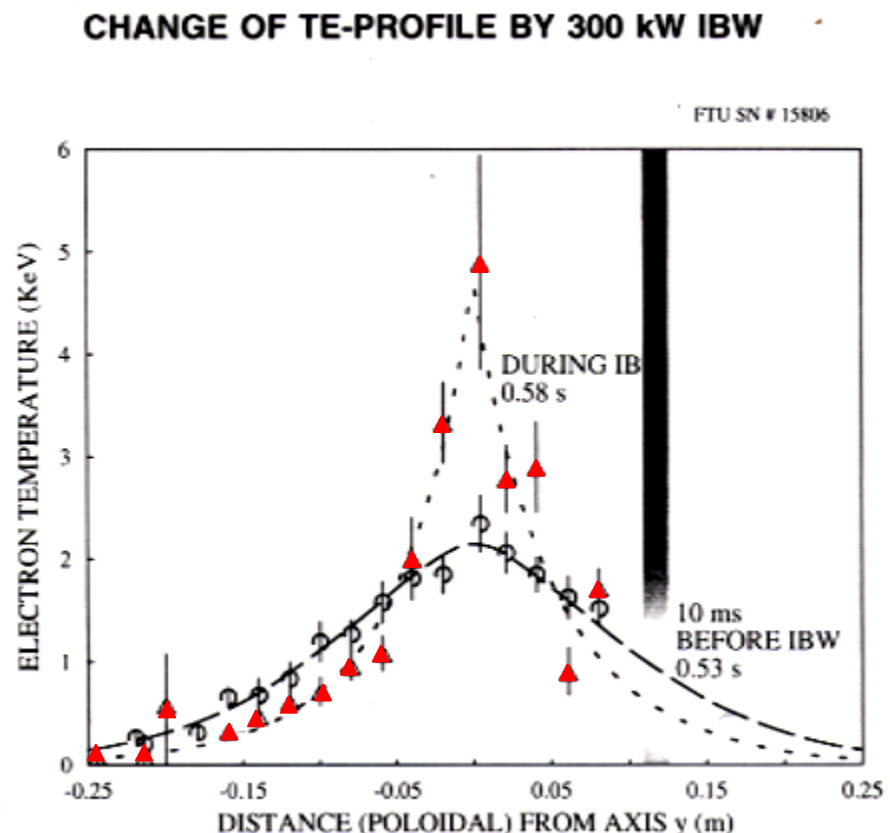


TFTR IBW Results

- Observed V_θ shearing during IBW coupling.
- Reynolds stress can explain the difference in behavior of experimental V_θ at different tritium densities.
- Did not observe creation of internal transport barrier:
 - V_θ shearing rate from carbon: $2.7 \times 10^4 \text{ s}^{-1}$
 - Growth rate (gyrofluid): $6.2 \times 10^4 \text{ s}^{-1}$
- Unresolved issue of time evolution

Internal Transport Barrier Observed on FTU

- 433 MHz, 7.9 T, $4\Omega_H$
- T_e heating/peaking
- Density peaking
- Consistent with internal transport barrier created by IBW
- R. Cesario, RF Conf. Annapolis, 1999

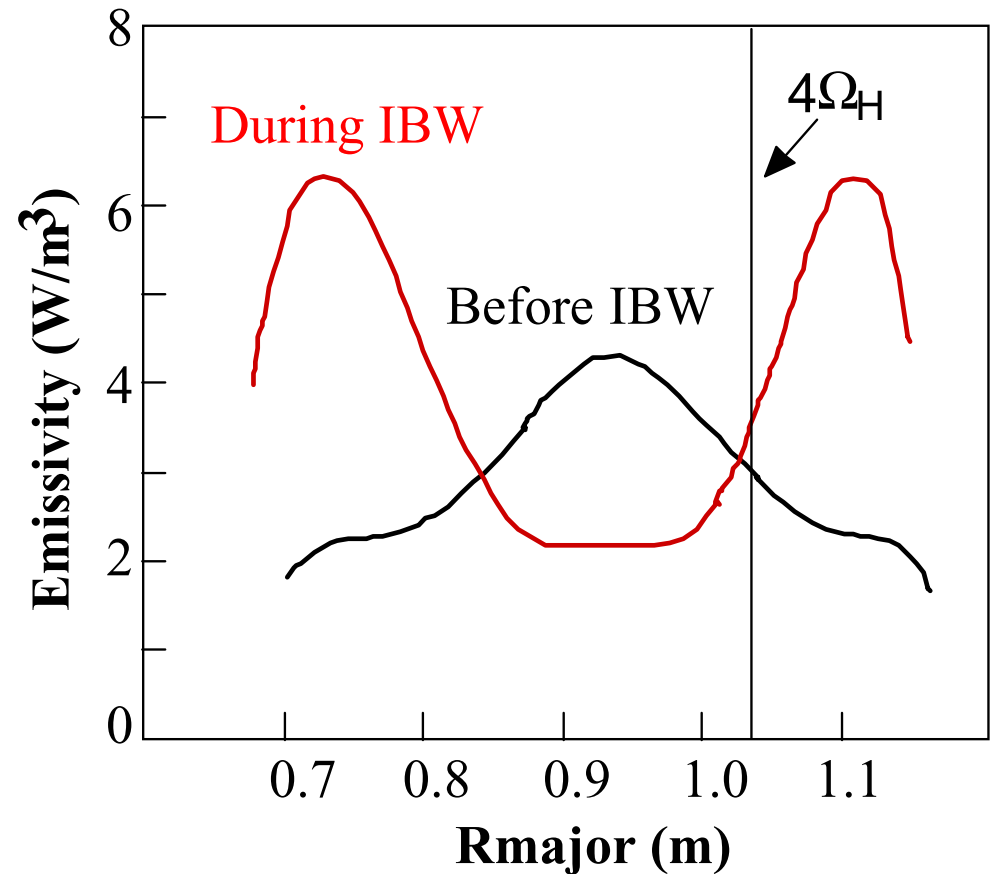


- $\Delta T_e \approx 2\text{keV}$

FTU

Impurity Penetration Impeded during IBW

- Impurity kept out of transport barrier
- Maximum of bolometric radiation moves out of the $4\Omega_H$.



FTU

FTU Results and IBW System

- Data consistent with heating and creation of transport barrier
- Have coupled up to 500 kW.
- Transport analysis indicate reduced diffusivity in the core region.
- FTU system is capable of 1.8 MW source power
 - frequency = 433 MHz
 - power source = klystron
 - 3 sources at a power of 600 kW each
 - pulse length = 1 s

FTU

Conclusion

- Reynolds stress explains salient features of the experimental V_θ observations on TFTR.
- Multi-species effects play an important role.
- FTU and PBX-M have observed internal transport barrier during IBW heating.
- IBW offer a means of controlling the pressure profile locally via poloidal drive, applicable to advanced tokamak or reactor.

Acknowledgements

R.E. Bell, M. Beer, S. Bernabei,
R. Cesario (ENEA-Frascati), J.C. Hosea,
R. Majeski, M. Ono, C.K. Phillips,
G. Schilling, C.H. Skinner, J.R. Wilson